

Local diurnal upwelling driven by sea breezes in northern Monterey Bay

C.B. Woodson^{a,*}, D.I. Eerkes-Medrano^b, A. Flores-Morales^c, M.M. Foley^d,
S.K. Henkel^e, M. Hessing-Lewis^b, D. Jacinto^f, L. Needles^e, M.T. Nishizaki^g,
J. O'Leary^d, C.E. Ostrander^a, M. Pespeni^h, K.B. Schwagerⁱ, J.A. Tyburczy^b,
K.A. Weersing^a, A.R. Kirincich^j, J.A. Barth^j, M.A. McManus^a, L. Washburn^k

^aDepartment of Oceanography, University of Hawai'i at Manoa, Honolulu, HI, USA

^bDepartment of Zoology, Oregon State University, Corvallis, OR, USA

^cCICESE, Ensenada, B.C., Mexico

^dEcology and Evolutionary Biology, University of California, Santa Cruz, CA, USA

^eEcology, Evolution and Marine Biology, University of California, Santa Barbara, CA, USA

^fCIEMAR, Universidade de Évora, Sines, Portugal

^gDepartment of Biology, University of Washington, Seattle, WA, USA

^hHopkins Marine Station, Stanford University, Monterey, CA, USA

ⁱInterdepartmental Graduate Program in Marine Science, University of California, Santa Barbara, USA

^jCOAS, Oregon State University, Corvallis, OR, USA

^kGeography Department, University of California, Santa Barbara, CA, USA

Received 24 January 2007; received in revised form 21 May 2007; accepted 23 May 2007

Available online 13 June 2007

Abstract

Sea breezes often have significant impacts on nearshore physical and biological processes. We document the effects of a diurnal sea breeze on the nearshore thermal structure and circulation of northern Monterey Bay, California, using an array of moorings during the summer upwelling season in 2006. Moorings were equipped with thermistors and Acoustic Doppler Current Profilers (ADCPs) to measure temperature and currents along the inner shelf in the bay. Temperature and current data were characteristic of traditional regional scale upwelling conditions along the central California coast during the study period. However, large diurnal fluctuations in temperature (up to 5 °C) were observed at all moorings inshore of the 60-m isobath. Examination of tidal, current, temperature, and wind records revealed that the observed temperature fluctuations were the result of local diurnal upwelling, and not a result of nearshore mixing events. Westerly diurnal sea breezes led to offshore Ekman transport of surface waters. Resulting currents in the upper mixed layer were up to 0.10 m s⁻¹ directed offshore during the afternoon upwelling period. Surface water temperatures rapidly decreased in response to offshore advection of surface waters and upwelling of cold, subsurface water, despite occurring in the mid-afternoon during the period of highest solar heat flux. Surface waters then warmed again during the night and early morning as winds relaxed and the upwelling shadow moved back to shore due to an unbalanced onshore pressure gradient.

*Corresponding author. Tel.: +1 4043075331.

E-mail address: cwoodson@hawaii.edu (C.B. Woodson).

Examination of season-long, moored time series showed that local diurnal upwelling is a common, persistent feature in this location. Local diurnal upwelling may supply nutrients to nearshore kelp beds, and transport larvae to nearshore habitats. Published by Elsevier Ltd.

Keywords: Upwelling; Sea breeze; Diurnal; Larval transport; Ekman transport

1. Introduction

Upwelling and relaxation are important physical processes that can have significant impacts on primary production, larval recruitment, and fisheries (Traganza et al., 1987; Roughgarden et al., 1991; Rau et al., 2001). Regional scale (100s of km) wind forcing along the eastern subtropical Pacific coast fluctuates between upwelling favorable and relaxation conditions at periods between 15 and 40 days during the spring upwelling season (e.g., Breaker and Broenkow, 1994). During upwelling favorable conditions, winds are northwesterly leading to offshore Ekman transport and a predominance of cold, nutrient rich waters close to the coast. Brief periods of wind relaxation allow warm offshore waters in the California Current to move back toward the coast. This upwelling/relaxation cycle has been linked to recruitment pulses of both intertidal invertebrates and commercially important fish species (Wing et al., 1995; Rau et al., 2001). However, local wind forcing (10s of km) may significantly alter regional forcing at smaller spatial and temporal scales (Kaplan et al., 2003; Drake et al., 2005).

Interactions between upwelling favorable winds and coastal topography produce an upwelling center north of Monterey Bay at Point Año Nuevo (Rosenfeld et al., 1994; Fig. 1). The upwelling plume then extends offshore, but also extends south across the mouth of Monterey Bay isolating surface waters within the bay from offshore waters (Rosenfeld et al., 1994). As a result, a warm upwelling shadow develops in the north-northeastern portions of Monterey Bay (Fig. 1; Graham, 1993). Surface temperatures in the upwelling shadow can be greater than 17 °C compared to recently upwelled waters, which average 10 °C. The lens of warm water (or upwelling shadow) typically extends to between 4 and 7 m depth. Hence, the upwelling shadow is characterized by intense stratification in the upper water column with cool waters below the warm surface layer. Stratification within the upwelling shadow is conducive to internal waves, internal tides, solitons (or solitary-like waves), and tidal

bores that can occur at temporal scales from several minutes to a few days (Petruncio et al., 1998; Carter et al., 2005; McManus et al., 2005). Northwestward currents dominate the flow patterns alongshore in northern Monterey Bay, in contrast to predominant southward currents in the upwelling plume (Storlazzi et al., 2003; Drake et al., 2005).

Regional scale upwelling is driven by northwesterly winds from the north Pacific high. These offshore winds are relatively consistent and do not show a diurnal period (Beardsley et al., 1987). However, in northern Monterey Bay, strong daily solar heating in the Salinas Valley to the south-southeast causes strong westerly diurnal sea breezes (Fig. 1; Banta et al., 1993). These winds can significantly affect nearshore circulation at temporal scales greater than 24 h (Beardsley et al., 1987; Rosenfeld, 1988; Drake et al., 2005). The diurnal response of current speeds to the afternoon sea breeze can be two to three times greater than the average values along the inner shelf (Rosenfeld, 1988). Because of the east–west orientation of the coast in northern Monterey Bay (e.g., east–west, Fig. 1), these winds should also lead to offshore Ekman transport.

Previous studies of the upwelling shadow and local wind forcing have focused on temporal scales of longer than a day and thus have not examined diurnal wind effects on inner shelf circulation (e.g., Graham and Largier, 1997; Drake et al., 2005). Here, we expand on previous efforts by examining diurnal winds and their effects on local upwelling circulation. We also speculate on the consequences of this circulation for nutrient delivery and larval transport.

2. Methods

Instrumentation used in this study consisted of four inner-shelf moorings (depths less than 30 m) and two mid-shelf moorings located in northern Monterey Bay, just off the coast from Long Marine Lab (Fig. 1, LML, University of California, Santa Cruz). Three moorings located at the 18, 60, and 100 m isobaths (Fig. 1; TPT001, TPT007, and

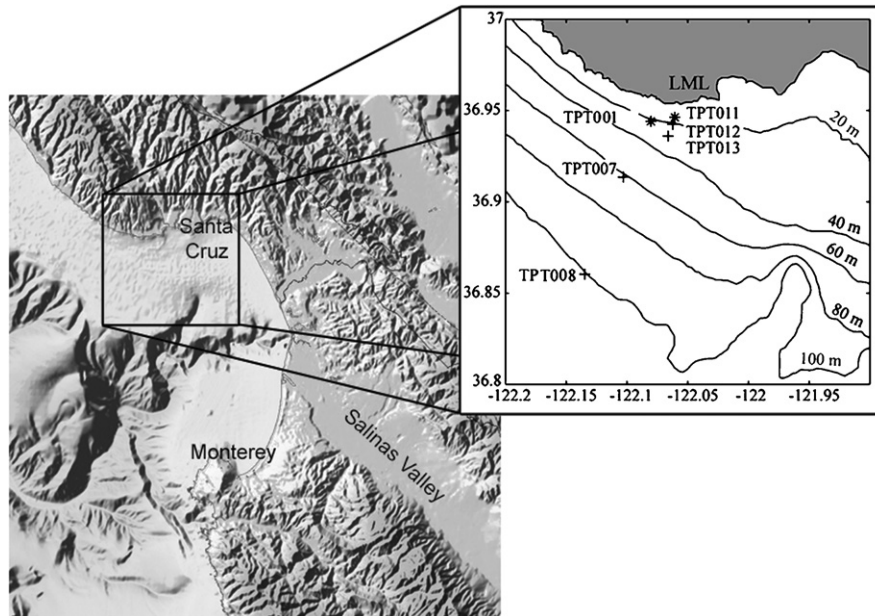


Fig. 1. Map of Monterey Bay showing the study area, the location of the ADCPs, and thermistor chains + indicates location of thermistor chain only. * indicates location of thermistor chain and ADCP.

Table 1
Mooring locations, instrument types, and depths for long-term and short-term deployments

Mooring ID	Water depth (m)	Latitude (°N)	Longitude (°W)	Thermistor depths (m)	ADCP range (m)	Major (y-) axis (deg)
<i>Seasonal data</i>						
TPT001	18	36.94	122.08	0, 5, 11, 17	3–15	296
TPT007	60	36.92	122.10	0, 5, 10, 20, 40, 60	–	
TPT008	100	36.86	122.13	0, 6, 10, 20, 40, 60, 100	–	
<i>High spatial-resolution data</i>						
TPT011	10	36.95	122.06	0, 4, 6, 7, 8, 9	2–7	268
TPT012	18	36.94	122.06	0, 4, 7, 11, 14, 17	–	
TPT013	30	36.94	122.07	0, 4, 7, 11, 14, 17, 21, 25, 29	–	

Major-axis is reported for the depth averaged flow.

TPT008, respectively) are part of the Partnership for Interdisciplinary Studies of Coastal Ocean's (PISCO) long-term monitoring program and were deployed for the duration of the analysis period covering 31 March–17 July 2006. Hereafter these are referred to as the 'seasonal' moorings. The study period captures most of the summer upwelling season (Largier et al., 1993; Breaker and Broenkow, 1994). Three additional nearshore moorings located approximately 1.6 km to the east of the seasonal moorings at the 10, 18, and 30 m isobaths (Fig. 1; TPT011, TPT012, TPT013, respectively) were de-

ployed for higher frequency, and higher spatial-resolution time records from 22 June to 1 July 2006. Hereafter, these moorings are referred to as the 'high resolution' moorings. Thermistors were located on each of the moorings at depths specified in Table 1 and recorded temperature at 30, 120, or 240 s intervals using either StowAway Tidbits or XTI temperature loggers (Table 1, Onset Computer Corp.). XTI loggers were encased in PVC housings with a stainless steel external probe yielding a response time of 30 s. StowAway Tidbits were deployed in a standard fashion with response times

on the order of a few minutes. Currents were measured through the water column with bottom-mounted, upward-looking 600-kHz Workhorse Sentinel acoustic Doppler current profilers (ADCPs, RDI Instruments) at TPT011 and TPT001 for both high spatial resolution and seasonal data records. ADCPs recorded current velocities at 30 and 120 s for high spatial-resolution and seasonal deployments, respectively. Regional data were obtained for both winds (NDBC mooring 46042, NOAA) and sea surface temperature (SST, NOAA). Regional surface current data were collected by land-based high-frequency coastal radar using CODAR system (Paduan and Shulman, 2004). Local wind data were obtained every 5 min from LML (approximately 1.1 km north of TPT001 at 36.95°N, 122.07°W, 25 m elevation, Fig. 1).

Wind, temperature, and current velocity data were low-pass filtered with a half-power period of 6 h with the exception of data being used to calculate the Richardson number (Ri). Temperature and ADCP data records were chosen to minimize data gaps. The few remaining gaps were filled using low-pass filtered white noise with mean and variance matching upwelling season statistics. Data gaps were less than 2 days long. Seasonal mooring data were divided into three 54-day sub-windows with a 50% overlap, detrended using a linear fit to each sub-window, and multiplied by a Hanning window to compute power spectra. Similar procedures were used for coherence and phase calculations between LML wind and seasonal current and temperature data. Statistical significance in coherence was calculated with the Goodman formula using the same methods as Drake et al. (2005), Harris (1978), and Thompson (1979).

3. Results

Regional conditions during the study period (31 March–17 July 2006) were typical of the spring upwelling season for the central California Current (Fig. 2; Skogsberg, 1936; Largier et al., 1993). The spring transition to the upwelling season is evident between 5 and 10 April 2006 with northwesterly winds dominating the time record for the remainder of the study period (Fig. 2b, spring transition indicated by vertical line). Four distinct relaxation periods lasting from 3 to 7 days occurred during the seasonal data record. East–west wind velocity at LML showed distinct periods of strong upwelling favorable winds with a diurnal cycle (e.g. 29 June

through 6 July, Fig. 2c). Similar diurnal cycles were observed at the M0 CIMT (36.83°N, 121.85°W; Center for Integrated Marine Technology) mooring maintained by Monterey Bay Aquarium Research Institute (MBARI). The M0 mooring is on a direct line between our site and the Salinas Valley to the southeast (Fig. 1). However, due to orographic steering near the coast, we report only the local LML winds here. Surface temperatures at the three long-term moorings were around 12°C during upwelling conditions and warmed to near 15°C during wind relaxation. This temperature pattern is characteristic of regional upwelling conditions within Monterey (Fig. 2d–f; Breaker and Broenkow, 1994).

The 5-m temperature logger at the 100-m isobath (TPT008) showed marked cooling in the upper water column during upwelling favorable winds indicating that it was in the upwelling plume at these times (Fig. 2f). In contrast, this mooring was in warmer offshore waters during relaxation periods. Nearshore moorings at the 18- and 60-m isobaths showed similar patterns with respect to regional upwelling/relaxation (Fig. 2d and e). However, moorings at 18 and 60 m (TPT001 and TPT007) showed significant warming in near surface waters during upwelling conditions (less than 7 m depth) consistent with the developing upwelling shadow. During relaxation periods, TPT001 and TPT007 experienced a brief cooling period as the upwelling plume moved onshore, then a general warming pattern consistent with regional scale relaxation events (Fig. 2). Also evident at TPT001 and TPT007 are large diurnal temperature fluctuations of the same magnitude as seasonal and upwelling/relaxation variations (e.g. up to 5°C; Fig. 2d and e). These fluctuations are not evident at the 100 m mooring located within the Pt. Año Nuevo upwelling plume (TPT008; Fig. 2f).

Power spectra of the seasonal temperature records at the surface and 5 m depth at TPT001 and TPT007 show that significant peaks occur at diurnal and semi-diurnal frequencies (Fig. 3a–d). In contrast, these peaks are not evident at TPT008 farther offshore (Fig. 3e and f). The spectral amplitudes of the diurnal peaks are much larger than lower frequency amplitudes for low-frequency fluctuations from the 18-m isobath mooring and at least twice that of the semi-diurnal peaks. Seasonal data records also revealed that the diurnal fluctuations were not in phase with tidal cycles. Temperature records also did not show a characteristic asymmetric

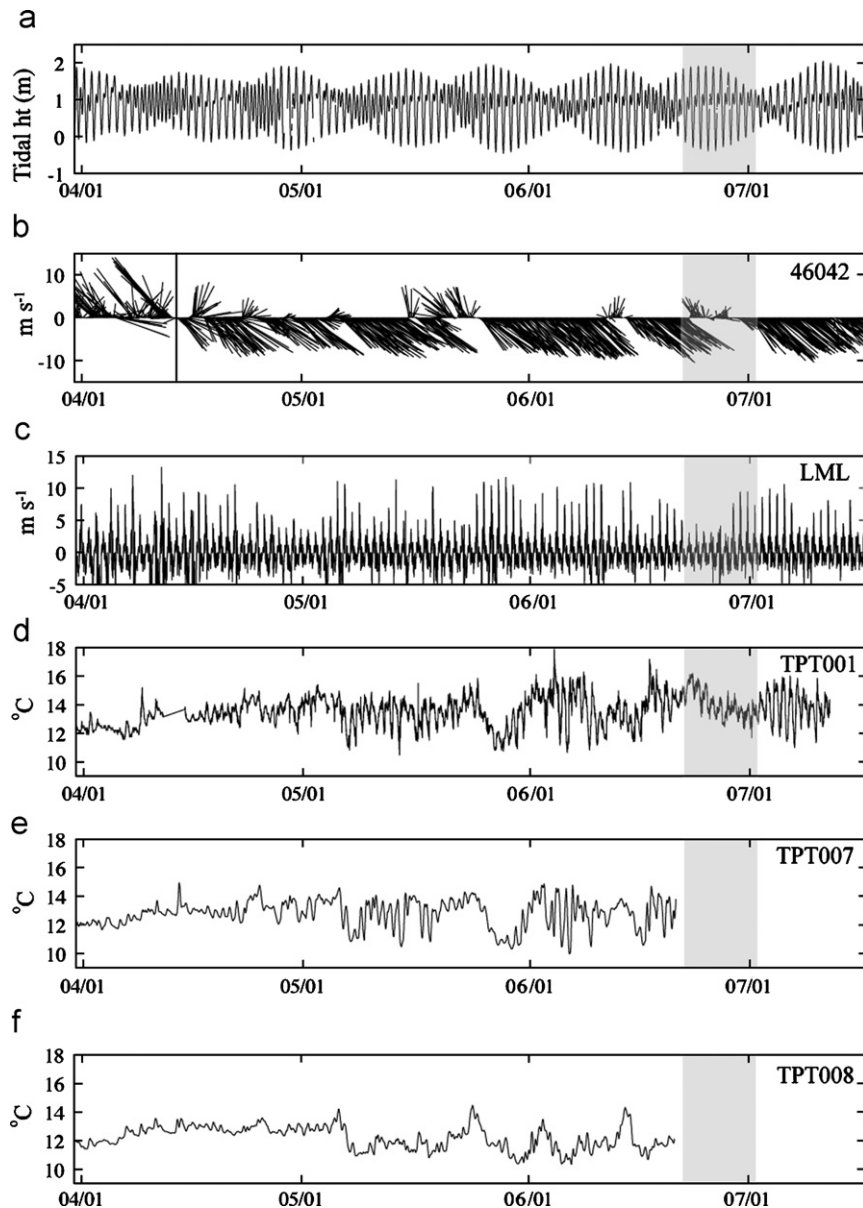


Fig. 2. Time-series of data between 31 March and 17 July 2006: (a) hourly tidal height (m) from the NOS Monterey Station; (b) hourly wind speed and direction from the NDBC buoy (spring transition indicated by vertical line); (c) East–west component of LML winds; (d) temperature at 5 m from TPT001; (e) temperature at 5 m from TPT007; (f) temperature at 6 m from TPT008. Shaded region shows the period of the high spatial-resolution deployment.

shape followed by internal waves, and current velocities recorded by ADCP did not increase on time scales of minutes as expected from tidal bores (Cairns, 1967; Winant, 1974; Pineda, 1991, 1994). Further, the diurnal period is outside of the internal waves pass band in Monterey Bay (~ 19.7 h).

To assess the influence of tides on the observed temperature variations, we conducted a tidal harmonic analysis on the temperature records from

the 18- and 100-m isobath moorings (TPT001 and TPT008, respectively) using the T_TIDE program (Pawlowicz et al., 2002). We compared the magnitude of variation for the diurnal and semi-diurnal tidal constituents to previously reported data (e.g., Petrucio et al., 1998). Table 2 shows the amplitude of the temperature perturbations assigned to seven major tidal constituents. The amplitude of the K1 period temperature fluctuations is greater than the

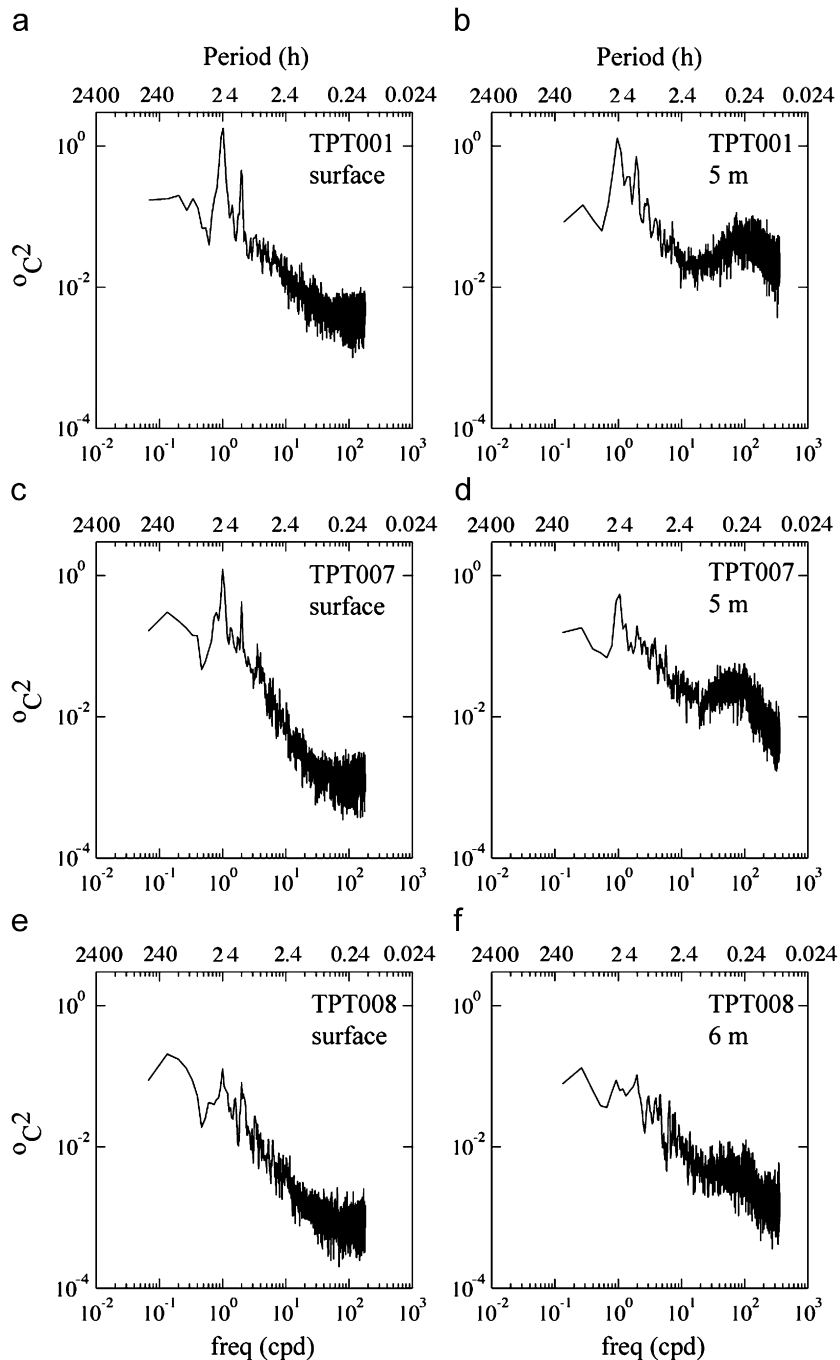


Fig. 3. Variance-conserving power spectra of long-term temperature data from Terrace Point: (a–b) surface and 5 m depth at TPT001, (c–d) surface and 5 m depth at TPT007, and (e–f) surface and 5 m depth at TPT008 respectively.

M2 period temperature fluctuations even though both the barotropic (i.e. sea level) and baroclinic (internal) M2 tides are larger than the K1 tides.

Hourly averaged winds and temperature contours are plotted for the high-resolution deployment in Fig. 4. During the high-resolution period, the

upwelling shadow extended to between 5 and 7 m depth with warm waters near 17°C in the upper layer and cooler waters at depth. The high-resolution data record captured a regional scale relaxation event from 24 to 29 June (Fig. 2b) when surface waters cooled, but remained stratified within the

Table 2

Tidal temperature variation at 1 m.a.b. from TPT001 and TPT008 for the spring upwelling season (31 March 17 July, 2006)

Tidal constituent	Frequency (cph)	Period (h)	TPT001 amplitude (°C)	TPT008 amplitude (°C)
O_1	0.0387	25.819	0.079 ± 0.13	0.035 ± 0.05
K_1	0.0417	23.934	0.613 ± 0.15	0.138 ± 0.07
N_2	0.0789	12.658	0.003 ± 0.11	0.013 ± 0.03
M_2	0.0805	12.421	0.070 ± 0.13	0.027 ± 0.03
L_2	0.0820	12.192	0.149 ± 0.17	0.004 ± 0.02
S_2	0.0833	12.000	0.202 ± 0.18	0.077 ± 0.03
SN_4	0.1623	6.1602	0.021 ± 0.05	0.005 ± 0.01

Temperature measurements are shown with standard error.

upwelling shadow. The diurnal sea breeze signal is evident in the latter part of the wind record (Fig. 4a). Local response of the ocean to the diurnal sea breeze led to surfacing of cool waters during afternoon hours between June 29 and July 1 at all three moorings. Closer examination of the east–west component of the diurnal sea breeze and temperature fluctuations at the 10-m isobath mooring (TPT001) suggest a strong linkage between LML winds and water temperature at this site (Fig. 5). Fig. 5 is plotted in local time (PDT) and night periods are shaded for interpretation. Each afternoon, water temperatures at 1 m.a.b. (meter above bottom) drop by close to 2 °C soon after the diurnal sea breeze reaches maximum speeds (Fig. 5c).

Three distinct periods based on the diurnal sea breeze cycle are evident in Fig. 5 and are similar to the divisions provided by Imberger (1985) for the diurnal mixed layer. These were defined as a morning period, an afternoon upwelling period, and a night relaxation period. Table 3 shows mean temperature differences for each period from the long-term temperature moorings and suggest diurnal upwelling.

Water column velocity profiles from ADCPs at both 10- and 18-m isobaths (TPT011 and TPT001, respectively) are plotted in Fig. 6 using the divisions established by Imberger (1985). Afternoon upwelling period profiles indicate wind-driven upwelling with surface waters moving offshore and return flow at depth. The region of highest shear at both sites also coincides with the depth of the upwelling shadow (~4–7 m). Richardson numbers ($Ri = N^2 / (du/dz)^2$) throughout the study period were always much greater than 0.25 suggesting a stable water column state conducive to upwelling baroclinic flow generation, and commonly observed in the northern Monterey Bay upwelling shadow. Current profiles for the night and morning periods suggest onshore

transport of the upwelling shadow. This diurnal process is reminiscent of regional scale upwelling/relaxation but occurs at smaller scales and higher frequency within the upwelling shadow (order of 10 km and 24-h period). Northwestward currents in the region lead to a net northwestward transport of water (Drake et al., 2005).

Both cross-shelf currents and temperature showed significant coherence with LML winds (Fig. 7). Local winds led cross-shelf currents by 2.66 h and led surface temperatures by 7.22 h. The 2.66-h lag between currents and local winds is consistent with the local spin-up of Ekman transport (Ekman, 1905). The larger lag from surface temperatures is believed to be the result of the time necessary for cooler waters below the upwelling shadow (~7 m depth) to reach the surface once offshore Ekman transport has been established. Taking both the depth of the upwelling shadow and the difference in wind-current and wind-temperature lags yields vertical velocities in the nearshore around 0.00043 m s^{-1} (37.15 m day^{-1}).

Wind stress during the afternoon upwelling period was used to estimate Ekman transport velocities during the afternoon upwelling period on June 30. This date was representative of local upwelling conditions. These velocities were then used to estimate the distance the upwelling shadow was advected offshore. Ekman transport velocities were calculated as $u = \tau / (\rho_w f d)$, where u is the depth-averaged velocity in the upper layer, τ is the wind stress calculated from Large and Pond (1981), ρ_w is the density of seawater (1026 kg m^{-3}), f is the Coriolis parameter ($1.39 \times 10^{-5} \text{ s}^{-1}$), and d is the upper layer depth (7 m). Although this estimate may overestimate velocities over the inner shelf, it does provide a useful upper bound for comparison to measured currents (Kirincich et al., 2005). Measured winds yield offshore current velocities in the

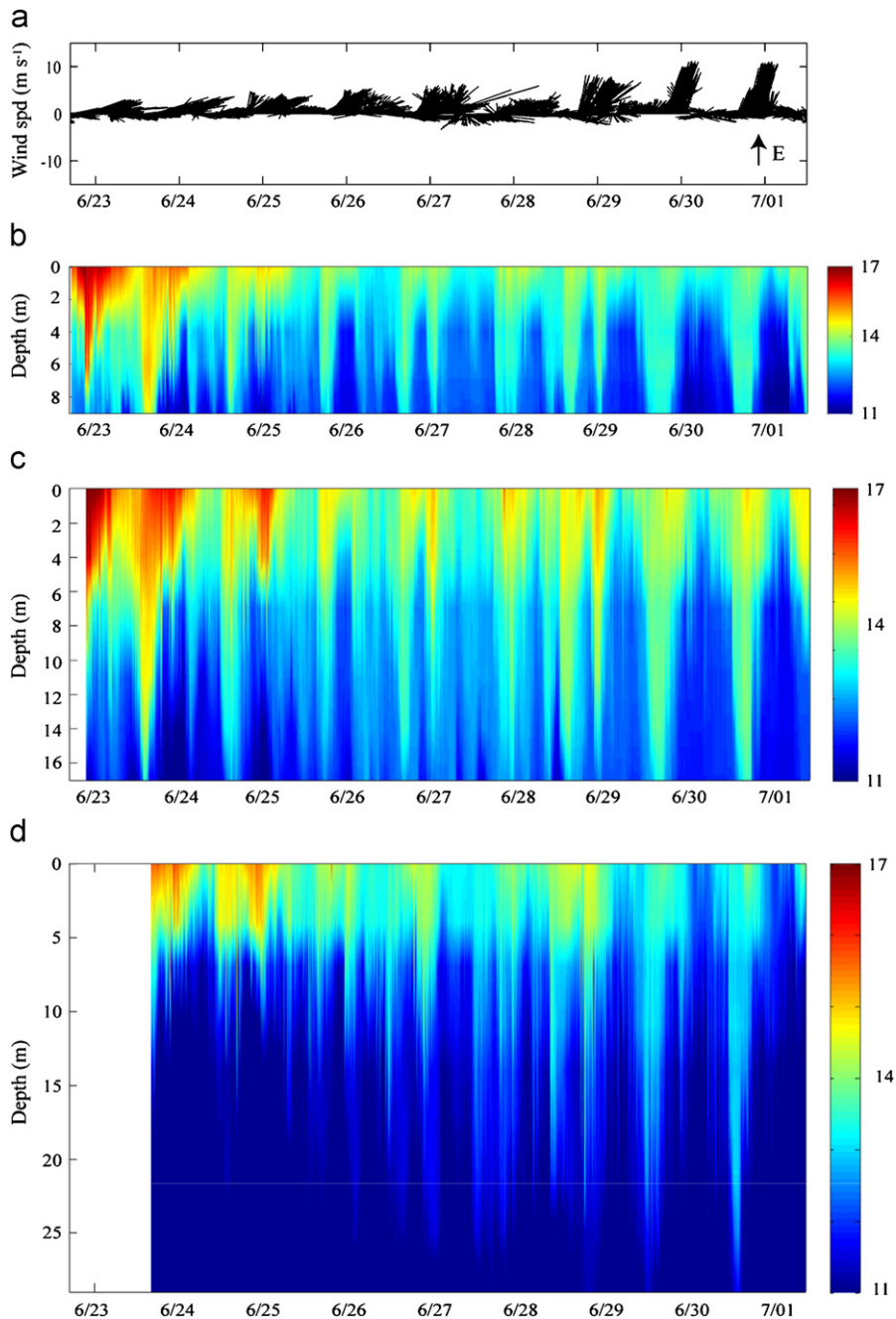


Fig. 4. Nine-day nearshore oceanographic data record at Terrace Point: (a) 5-min vector winds from LML (east is up); (b–d) temperature record at TPT011 (10 m water depth), TPT012 (18 m water depth), TPT013 (30 m water depth).

upper few meters of the water column between 0.029 and 0.094 m s^{-1} during afternoon hours with sustained westerly winds over 3 m s^{-1} . On July 30, offshore flow in the upper water column peaked at 0.079 m s^{-1} at about 1930 local time (PDT), began to subside at 2200 and reversed direction by 2300 in

agreement with Ekman transport estimates (Fig. 8). Onshore flow at depth compensates for the strong offshore Ekman transport. Using this theory over 6 h of sustained upwelling favorable winds, the upwelling front would travel up to 3 km offshore. The location of TPT013 at $\sim 1700 \text{ m}$ from shore

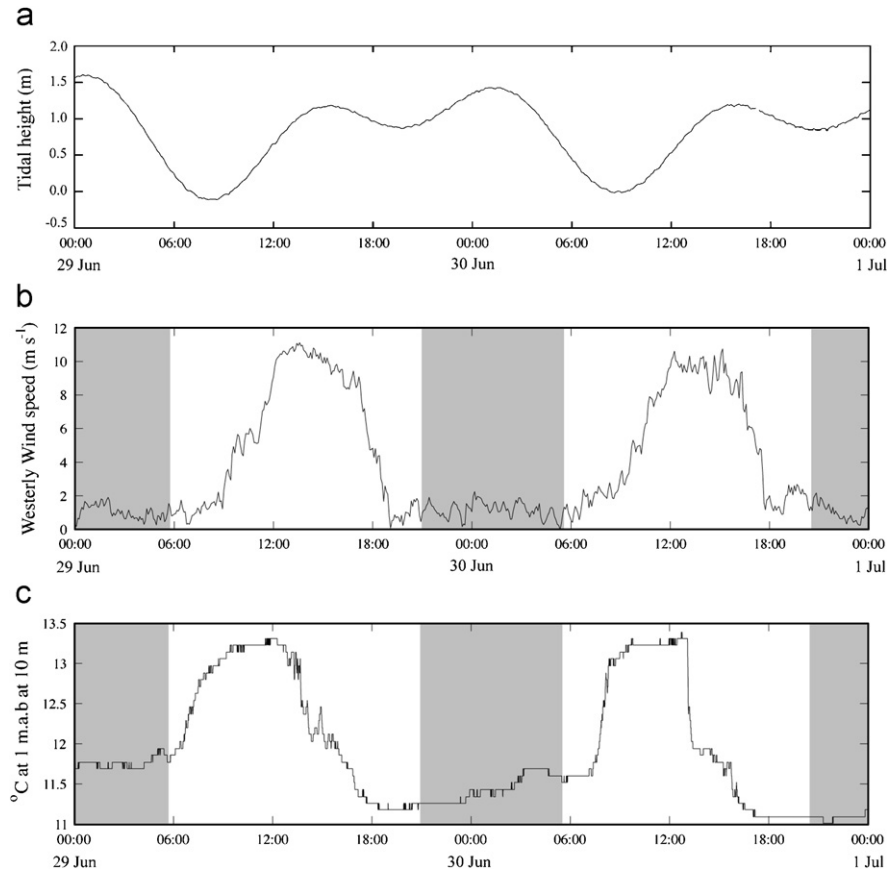


Fig. 5. Local winds at LML and temperature at TPT011 (1 m.a.b.) plotted in local time showing sunrise and sunset (shaded).

Table 3

Mean temperature at TPT001 during diurnal upwelling event (1 July–13 July, 2006) for three periods during the day

Period	Span	Surface (°C)	5 m (°C)	11 m (°C)	Bottom (°C)
Night relaxation	1800–0200	14.31 ± 0.26	12.22 ± 0.33	11.02 ± 0.31	10.45 ± 0.22
Morning	0200–1000	14.62 ± 0.37	12.82 ± 0.22	11.36 ± 0.27	10.78 ± 0.26
Afternoon upwelling	1000–1800	12.47 ± 0.33	11.58 ± 0.25	10.61 ± 0.23	10.22 ± 0.22

All measurements are shown with standard error.

verifies this analysis as the upwelling front only crossed this mooring on high-wind days during the end of the 1-week observation period (Fig. 4d).

We incorporated daily cooling due to mixing during the night relaxation period into the residence time analysis of Graham and Largier (1997) for the upwelling shadow. Surface heating in the upwelling shadow has been estimated at $0.54\text{ }^{\circ}\text{C day}^{-1}$ (Rosenfeld et al., 1994; Graham and Largier, 1997; Beardsley et al., 1998). Diurnal upwelling and cooling due to mixing during the night and morning relaxation periods lead to a reduction in the daily

warming of the upwelling shadow from 0.54 to $0.39\text{ }^{\circ}\text{C day}^{-1}$ or roughly 27%. The reduction in warming leads to a decrease in the realized value of the heat flux, Q , of 27% because heat is transferred to depth and not fully retained in the surface layer. Inserting the reduced value for Q within the upwelling shadow into the residence time calculation as

$$R = \rho c H \Delta T / Q, \quad (1)$$

where $\rho = 1026\text{ kg m}^{-3}$, $c = 3993\text{ J kg}^{-1}\text{ }^{\circ}\text{C}^{-1}$, $Q = 0.180\text{ kW m}^{-2}$, $H = 7\text{ m}$, and ΔT is the change in

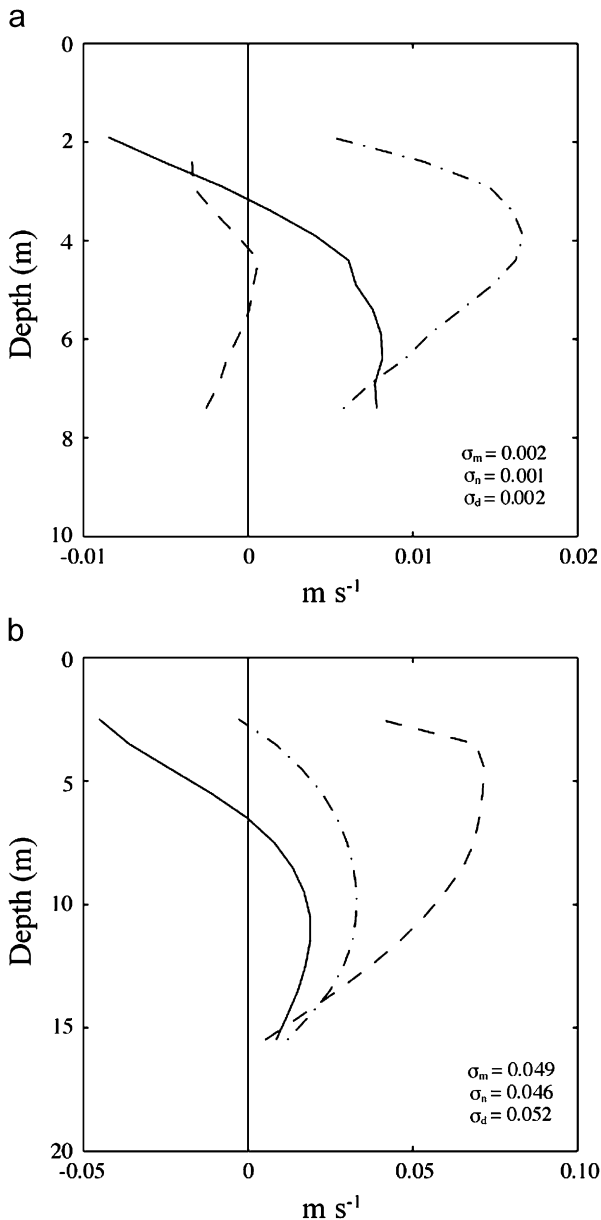


Fig. 6. Mean 8-h cross-shelf velocity profiles (positive onshore) from ADCP during 23 June–2 July 2006: (a) TPT011; (b) TPT001. Each line represents a distinct 8-h period: afternoon upwelling (solid), night relaxation (dashed), and morning relaxation (dash dot).

temperature between the offshore upwelling plume (8–10 °C) and within the upwelling front (up to 17 °C), yields an increase in residence time for waters within the upwelling shadow from 8 days as estimated by [Graham and Largier \(1997\)](#) to 13–17 days. Oceanographic and climatic variability within seasons and between years likely leads to a wide range of retention within the northern bay. Cooling

of surface waters due to diurnal upwelling thus increases residence time estimates within the upwelling shadow. Incorporating the results of [Graham and Largier \(1997\)](#) and results in this study, we suggest a new retention of 8–17 days within the northern bay.

4. Discussion

Large diurnal temperature fluctuations were observed in coastal waters in northern Monterey Bay. Similar diurnal variations were not present in the outer bay (within the upwelling plume) during the study period. The diurnal fluctuations could not be attributed solely to surface heating due to their large range (e.g., >4 °C at 5 m depth). Diurnal fluctuations are also greater than the Coriolis frequency at the latitude of our study (~19.7 h). In addition, the fluctuations were not the result of nearshore mixing events because the water column cooled to depth, Richardson numbers remained greater than 0.25 in the study region, and cross-isobath flow reversed direction with depth. Further analysis of the local wind field and nearshore, high-resolution temperature and current profile data suggested that local diurnal upwelling is the primary cause for the observed temperature fluctuations. Comparison to long-term temperature, wind, and current records showed that diurnal upwelling is a persistent feature in northern Monterey Bay that may have significant effects on local biological processes.

Wind forcing along the coast of California is a driving mechanism behind this biologically productive region ([Traganza et al., 1987](#); [Roughgarden et al., 1991](#); [Rau et al., 2001](#)). Offshore, upwelling favorable winds dominate the spring and summer seasons leading to increases in primary productivity and can have significant effects on local biota and commercial fisheries ([Traganza et al., 1987](#)). However, local dynamics on the inner shelf may be drastically different ([Drake et al., 2005](#)). During summer months, intense warming in the Salinas Valley to the southeast drives an alongshore sea breeze that develops through the afternoon before dying off just after dusk. The dominant eastward component of the sea breeze pushes the warm stratified waters of the upwelling shadow offshore up to 3 km each afternoon. The offshore movement of the upwelling shadow leads to large temperature drops in the surface waters during the middle of the day when solar heating is at its peak. As sea breezes

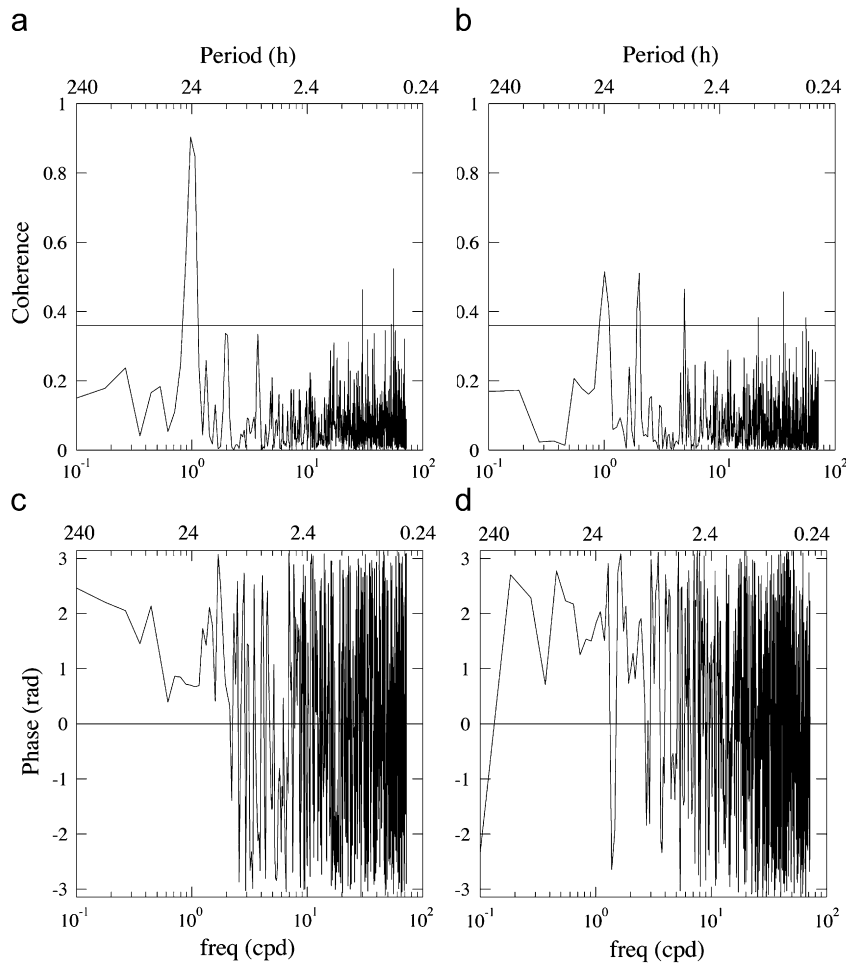


Fig. 7. Coherence and phase (radians) plots for east–west component of local winds vs. surface temperature (a, c) and cross-shelf current velocity (b, d) at 2.5 m bin depth. Coherence becomes significant above horizontal line at 99% confidence.

die down at dusk, offshore Ekman transport is reduced, and the upwelling shadow slowly returns to the coast resulting in overnight and early morning warming of surface waters by 1–3 °C likely due to an onshore pressure gradient created between the warm upwelling shadow and cool upwelled waters nearshore.

Warming of upwelled waters and surface heating in the upwelling shadow during regional upwelling conditions were estimated using the methods of Rosenfeld et al. (1994). Surface heat flux accounted for less than 1% of the differences in heat content between night and morning periods, as the total heat flux was minimal during early morning hours and overnight. Surface heating by solar radiation alone, therefore cannot explain the rapid increase in temperature suggesting advection of the upwelling

shadow back to shore as currents reverse (Rosenfeld et al., 1994).

Residence times in the upwelling shadow may be longer than previously estimated due to mixing between the regional upwelling shadow and recently upwelled waters nearshore. Using surface heat flux in a novel method, Graham and Largier (1997) estimated retention in the upwelling shadow of northern Monterey Bay at approximately 8 days. This residence time estimate suggested current velocities in the recirculation region of about 0.10 m s^{-1} . Data from this and a previous study (Drake et al., 2005) show that mean currents within the upwelling shadow are closer to 0.06 m s^{-1} resulting in residence times of closer to 13 days or more in the advection model proposed by Graham and Largier (1997). Our estimates of residence time

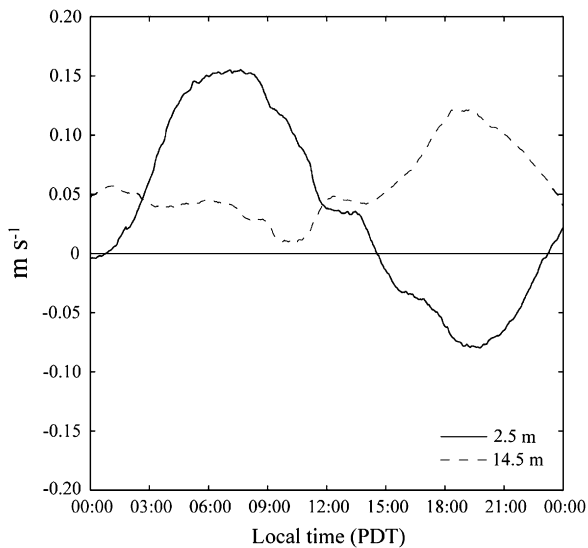


Fig. 8. Cross-shelf velocity (positive onshore) at TPT001 for 2.5 m (solid line) and 14.5 m (dashed line) depth on 30 July 2006 plotted in local time.

of 13–17 days incorporating cooling of the upwelling shadow due to diurnal upwelling are in agreement with these observations. Our results support the advective scenario proposed by [Graham and Largier \(1997\)](#), although changes in the local wind regime and physical oceanographic conditions are likely to cause significant variation around these residence time estimates. Residence times in northern Monterey Bay also may be significantly longer than current estimates (8–17 days) if surface waters circulate more than once.

Local diurnal upwelling is likely to influence the local biota through (1) delivery of nutrients to the nearshore kelp beds, (2) increasing retention times in the northern bay to overlap with the pelagic larval duration of many invertebrate larvae, and (3) providing a recurring larval transport mechanism ([Roughgarden et al., 1991](#); [Incze and Naimie, 2000](#); [Yannicelli et al., 2006](#)). The pulsed delivery of cold sub-thermocline waters to nearshore environments may provide nutrients to promote algal growth along the inner shelf ([Leichter et al., 1996, 2006](#)). Pulsed delivery of nutrients to kelp beds and planktonic communities in the California Current is an important source of resources for these habitats ([Shea and Broenkow, 1982](#); [Zimmerman and Kremer, 1984](#)). In addition to nutrient delivery, the diurnal movement of the upwelling shadow may concentrate larvae at the edge of the upwelling shadow. As a result, organisms in the water column

will be aggregated as the front moves offshore, then delivered to the intertidal during relaxation at dusk in much the same fashion as regional scale upwelling/relaxation events ([Roughgarden et al., 1991](#)). Local diurnal upwelling, however, occurs at local scales much like onshore translating internal tidal bores ([Pineda, 1991, 1999](#)). This sea breeze-driven transport mechanism insures that larvae arrive after dark and can thus avoid visual predators such as young-of-year rockfish (*Sebastes* spp.; [Gaines and Roughgarden, 1987](#)). Furthermore, it occurs independently of tide and moon phase. Local diurnal upwelling is however dependent on stratification within northern Monterey Bay and the local diurnal sea breeze, which can develop early during regional upwelling periods before a significant regional upwelling signal is observed.

5. Conclusions

The diurnal sea breeze and resulting response of the nearshore circulation raises questions about the importance of local processes on nearshore habitats. Previously, upwelling/relaxation was believed to be a regional scale event, whereas tidal bores and internal waves have been implicated at more local scales. The unique physical characteristics of the northern Monterey Bay upwelling shadow (e.g. intense stratification, or strong temperature gradient, with a shallow mixed layer) and the strong alongshore, diurnal sea breeze are conducive to diurnal upwelling that likely has significant impacts on local biota. The presence of a persistent local transport mechanism for nutrients and larvae may explain recruitment variability at local scales, and suggests that local nearshore oceanography may have significant influences on population dynamics and community structure in nearshore habitats.

Acknowledgments

This is contribution number 254 from PISCO, the Partnership for Interdisciplinary Studies of Coastal Oceans funded primarily by the Gordon and Betty Moore Foundation and the David and Lucile Packard Foundation. This project evolved as a culmination of an interdisciplinary training course taught through PISCO at UCSC. Student authorship is ordered alphabetically following C.B.W. The authors would like to express gratitude to Dr. P. Raimondi, R. Skrovan, J.D. Figurski, P.J. Drake,

and PISCO personnel at UCSC for guidance, keen insights, logistics, and access to long-term data.

References

- Banta, R.M., Oliver, L.D., Levinson, D.H., 1993. Evolution of the Monterey Bay sea-breeze layer as observed by pulsed Doppler lidar. *Journal of Atmospheric Science* 50, 3959–3982.
- Beardsley, R.C., Dorman, C., Friehe, C., Rosenfeld, L., Winant, C., 1987. Local atmospheric forcing during the Coastal Ocean Dynamics Experiments 1 and 2: 1. A description of the marine boundary layer and atmospheric conditions over a northern California upwelling region. *Journal of Geophysical Research* 92, 1467–1488.
- Beardsley, R.C., Dever, E.P., Lentz, S.J., Dean, J.P., 1998. Surface heat flux variability over the northern California shelf. *Journal of Geophysical Research* 103, 21533–21586.
- Breaker, L.C., Broenkow, W.W., 1994. The circulation of Monterey Bay and related processes. *Oceanography and Marine Biology Annual Review* 32, 1–64.
- Cairns, J.L., 1967. Assymetry of internal tidal waves in shallow coastal waters. *Journal of Geophysical Research* 72, 3563–3565.
- Carter, G.S., Gregg, M.C., Lien, R.-C., 2005. Internal waves, solitary-like waves, and mixing on the Monterey Bay shelf. *Continental Shelf Research* 25, 1499–1520.
- Drake, P.T., McManus, M.A., Storlazzi, C.D., 2005. Local wind forcing of the Monterey Bay area inner shelf. *Continental Shelf Research* 25, 397–417.
- Ekman, V.W., 1905. On the influence of the Earth's rotation on ocean-currents. *Arkiv for Matematik, Astronomi, och Fysik* 2, 1–52.
- Gaines, S., Roughgarden, J., 1987. Fish in offshore kelp forests affect recruitment to intertidal barnacle populations. *Science* 235, 479–481.
- Graham, W.M., 1993. Spatio-temporal scale assessment of an 'Upwelling Shadow' in northern Monterey bay, California. *Estuaries* 16, 83–91.
- Graham, W.M., Largier, J.L., 1997. Upwelling shadows as nearshore retention sites: the example of northern Monterey Bay. *Continental Shelf Research* 17, 509–532.
- Harris, F.J., 1978. On the use of windows for harmonic analysis with the discrete Fourier transform. *Proceedings of the IEEE* 66, 51–83.
- Imberger, J., 1985. The diurnal mixed layer. *Limnology and Oceanography* 30, 737–770.
- Incze, L.S., Naimie, C.E., 2000. Modeling the transport of lobster (*Homarus americanus*) larvae and postlarvae in the Gulf of Maine. *Fisheries Oceanography* 9, 99–113.
- Kaplan, D.M., Largier, J.L., Navarrete, S., Guinez, R., Castilla, J.C., 2003. Large diurnal temperature fluctuations in the nearshore water column. *Estuarine, Coastal, and Shelf Science* 57, 385–398.
- Kirincich, A.R., Barth, J.A., Grantham, B.A., Menge, B.A., Lubchenko, J., 2005. Wind-driven inner-shelf circulation off central Oregon during summer. *Journal of Geophysical Research* 110, C10S03.
- Large, W.G., Pond, S., 1981. Open ocean momentum flux measurements in moderate to strong winds. *Journal of Physical Oceanography* 11, 324–336.
- Largier, J.L., Magnell, B.A., Winant, C.D., 1993. Subtidal circulation over the Northern California shelf. *Journal of Geophysical Research* 98 (C10), 18147–18179.
- Leichter, J.J., Wing, S.R., Miller, S.L., Denny, M.W., 1996. Pulsed delivery of subthermocline water to Conch Reef (Florida Keys) by internal tidal bores. *Limnology and Oceanography* 41, 1490–1501.
- Leichter, J.J., Helmuth, B., Fischer, A.M., 2006. Variation beneath the surface: quantifying complex thermal environments on coral reefs in the Caribbean, Bahamas, and Florida. *Journal of Marine Research* 64, 563–588.
- McManus, M.A., Cheriton, O.M., Drake, P.J., Holliday, D.V., Storlazzi, C.D., Donaghay, P.L., Greenlaw, C.F., 2005. Effects of physical processes on structure and transport of thin zooplankton layers in the coastal ocean. *Marine Ecology Progress Series* 301, 199–215.
- Paduan, J., Shulman, I., 2004. CODAR data assimilation in the Monterey Bay area. *Journal of Geophysical Research* 109, C07S09.
- Pawlowicz, R., Beardsley, B., Lentz, S., 2002. Classical tidal harmonic analysis including error estimates in MATLAB using T_TIDE. *Computers and Geosciences* 28, 929–937.
- Petruncio, E.T., Rosenfeld, L.K., Paduan, J.D., 1998. Observations of the internal tide in Monterey Canyon. *Journal of Physical Oceanography* 28, 1873–1903.
- Pineda, J., 1991. Predictable upwelling and the shoreward transport of planktonic larvae by internal tidal bores. *Science* 253, 548–551.
- Pineda, J., 1994. Internal tidal bores in the nearshore: warm-water fronts, seaward gravity currents and the onshore transport of neustonic larvae. *Journal of Marine Research* 52, 427–458.
- Pineda, J., 1999. Circulation and larval distribution in internal tidal bore warm fronts. *Limnology and Oceanography* 44, 1400–1414.
- Rau, G.H., Ralston, S., Southon, J.R., Chavez, F.P., 2001. Upwelling and the condition and diet of juvenile rockfish: a study using ¹⁴C, ¹³C, and ¹⁵N natural abundances. *Limnology and Oceanography* 46, 1565–1570.
- Rosenfeld, L.K., 1988. Diurnal period wind stress and current fluctuations over the continental shelf off northern California. *Journal of Geophysical Research* 93, 2257–2276.
- Rosenfeld, L.K., Schwing, F.B., Garfield, N., Tracy, D.E., 1994. Bifurcated flow from an upwelling center: a cold water source for Monterey Bay. *Continental Shelf Research* 14, 931–964.
- Roughgarden, J., Pennington, J.T., Stoner, D., Alexander, S., Miller, K., 1991. Collisions of upwelling fronts with the intertidal zone: the cause of recruitment pulses in barnacle populations of central California. *Acta Oecologica* 12, 35–51.
- Shea, R.E., Broenkow, W.W., 1982. The role of internal tides in the nutrient enrichment of Monterey Bay, California. *Estuarine, Coastal, and Shelf Science* 15, 57–66.
- Skogsberg, T., 1936. Hydrography of Monterey Bay, California. Thermal conditions, 1929–1933. *Transactions of the American Philosophical Society* 29, 152pp.
- Storlazzi, C.D., McManus, M.A., Figurski, J.D., 2003. Long-term, high-frequency current and temperature measurements along central California: insights into upwelling/relaxation and internal waves on the inner shelf. *Continental Shelf Research* 23, 901–918.

- Thompson, R.O.R.Y., 1979. Coherence significance levels. *Journal of Atmospheric Science* 36, 2020–2021.
- Tragana, E.D., Redalje, D.G., Garwood, R.W., 1987. Chemical flux, mixed layer entrainment, and phytoplankton blooms at upwelling fronts in the California coastal zone. *Continental Shelf Research* 7, 89–105.
- Winant, C.D., 1974. Internal surges in coastal waters. *Journal of Geophysical Research* 79, 4523–4526.
- Wing, S.R., Botsford, L.W., Largier, J.L., Morgan, L.E., 1995. Spatial structure of relaxation events and crab settlement in the northern California upwelling system. *Marine Ecology Progress Series* 128, 199–211.
- Yannicelli, B., Castro, L.R., Valle-Levinson, A., Atkins, L., Figueroa, D., 2006. Vertical distribution of decapod larvae in the entrance of an equatorward facing bay of central Chile: implications for transport. *Journal of Plankton Research* 28, 19–37.
- Zimmerman, R.C., Kremer, J.N., 1984. Episodic nutrient supply to a kelp forest ecosystem in Southern California. *Journal of Marine Research* 42, 591–604.